Broadening sound absorption coefficient with Hybrid Resonances

F. Bucciarelli [(1)], M. Meo [(1)]
[(1)]University of Bath, Mechanical Engineering Department, Bath, United Kingdom

Abstract
In the last years, a great research effort has been focused on the noise mitigation at low frequencies. Membrane-type acoustic metamaterials (AMM) are one of the most promising solutions to meet the growing demand for low frequency sound absorbers. Typically, acoustic membrane absorbers require large back cavities to achieve low frequency sound absorption, which is usually categorised by a single narrow absorption peak. This paper presents an acoustic resonator unit cell, comprising of a thin elastic silicone plate with an air gap cavity with broadband absorption in a frequency range between 250-400Hz. The broadband and multiple peak sound absorption showed by the proposed resonator is due to hybrid resonances which occur in the frequency range due to coupling of the structural dynamic response of the plate with the acoustic response of the air cavity. A numerical model based on acoustic-structural interaction, validated for experimental data, has been used to explain how the broadening gain in the sound absorption level is strictly related to the hybrid resonances of the unit cell resonator. We demonstrated that hybrid resonances are a function of the geometrical parameters and the ratio between the Young's modulus and the density of the material plate, thus the proposed resonators absorption frequency range is tuneable at low frequencies allowing a wider broadband not achievable with acoustic membrane absorbers.

1. Introduction
Noise control and reduction has become an important factor in many fields, along with an increased focus on sound absorption and sound absorbing materials. In particular, researchers have concentrated on improving the performance of acoustic metamaterial at low frequencies. Usually sound absorption is the result of the dissipation of sound energy through different physical mechanisms, such as viscous dissipation. Sound is associated with small air displacement velocities and thus sound dissipation can be expressed as a quadratic function of the frequency [1]. As a consequence, absorption at low frequencies is considerable weaker compared to higher frequencies; this highlights one of the main limitations of porous absorbers. Another important parameter associated to the dissipated energy is the impedance mismatch between the air and the solid, as the total sound absorption is low if most of the incident sound wave is reflected at the solid-air interface. To diminish effects of impedance mismatch many researchers propose microperfored panels (MPP), which use both; the concept of resonance to dissipated the sound energy and designed back-cavities to better impedance match with air over a desired frequency range. MPPs are generally tuned around a resonance frequency, so they are characterized by a single narrow absorption peak around such frequency [2-3]. In order to overcome single absorption peaks, many approaches have been presented. Parallel or series arrangement of multiple MPP absorbers with different cavity depths shows better absorption properties when compared with single MPP absorber [4-5-6]. Different research work tried to combine MPPs with honeycomb structures [7-8] or with elastic membranes [9-10] which showed absorption increases over larger frequency ranges. In any case, the absorption performance of MPP absorbers are strictly related to the geometrical properties and broadband absorption at low frequencies can only be achieved with high absorber thickness which represents a considerable engineering constrain. This has led the researchers to develop new acoustic metamaterials (AMM) [11] with the aim of achieving negative effective modulus and/or negative

effective density. A particular type of AMMs membranes and plate type acoustic metamaterial which have relatively simple geometry and are generally light-weight and smaller compared with other absorbers [12]. Yang [13] first proposed a membrane-type AMM composed by a pre-stressed membrane decorated with an attached mass which allowed for double peaks in the transmission curve, related to the eigenmodes frequencies, and one dip in between due to the anti-resonance because the two eigenmodes were excited with opposite phase. The effect of the pretension, the mass, the geometry and the number of the attached masses has also been investigated by Naify [14-15]. Mei proposed a fixed rectangular membrane decorated with semi-circular iron platelets backed with an aluminium reflector which could yield almost 100% absorption at low frequencies within a narrow band. This so called "dark AMM"[16] converts the sound energy into elastic energy through a flapping motion of the platelets, while resonance frequencies where peak absorption occurs can be tuned by adjusting the weight of platelets. Ma [17] presented a membrane –type metasurface comprised of a circular membrane with a circular attached mass with sealed gas behind. In this case, a narrow peak with 50% absorption was achieved at low frequencies because the resonator surface became impedance-matched to air at certain frequencies, (due to hybrid resonances). Whilst these AMM induce negative effective density, Yang [18] proposed a new concept which showed both negative effective density and negative effective bulk modulus. When two membranes (top and bottom) each decorated with a mass are connected to a ring and fixed to a sidewall, two main resonances are identified: monopolar and dipolar resonances. In the frequency range where monopolar and dipolar resonances overlap double negativity can be achieved with consequent narrow absorption peaks at the resonance peaks.

Membrane or plate type unit cells proposed until now allow good sound absorption at low frequencies, however broadband absorption cannot be achieved because the narrow absorption peaks which characterized such absorber occurs around the resonance of the resonator itself.

In this paper, a membrane-type unit cell acoustic metamaterial is proposed which guarantees a low frequency broadband absorption in the frequency range 250-400 Hz with two main absorption peaks of 80% at 268Hz and 369 Hz. The unit cell includes a silicone membrane fixed on a rigid frame with an air cavity behind. A prototype has been manufactured and tested in an impedance tube test rig. Also a numerical model is presented based on the acoustic-structure response in terms of the combination of structural and acoustic mode shapes. The numerical model was validated through experimental data and used to understand the reasons behind the multiple peaks and broadband absorption of the AMM unit cell.

2. Theoretical Framework

Considering an elastic and flexible plate with an enclosed cavity, then the vibration of plate is perturbed by the fluid pressure loading and the acoustic filed in the cavity is influenced by the dynamic response of the plate. The coupled structural-acoustic response of the system can be explained in terms of a combination of structural and acoustic mode shapes.

The structural flexural vibration of flat thin plate can be described in the finite element matrix formulation, by the *n* ordinary differential equations [19-20-21]

$$[\boldsymbol{M}]\{\ddot{\boldsymbol{w}}(t)\} + [\boldsymbol{C}]\{\dot{\boldsymbol{w}}(t)\} + [\boldsymbol{K}]\{\boldsymbol{w}(t)\} = \{\boldsymbol{f}(t)\} \quad (1)$$

where $[\boldsymbol{M}]$, $[\boldsymbol{C}]$, $[\boldsymbol{K}]$ are respectively the global mass, damping and stiffness matrices, while $\boldsymbol{w}(t)$, $\boldsymbol{f}(t)$ are the column vectors with the nodal degrees of freedom and the nodal excitations generated by the transverse forces acting on surface elements.

The acoustic vibration of fluid in a rigid-walled cavity can be analysed following the equation of motion, which is expressed in finite element matrix formulation in terms of nodal pressure [22-23]

$$[\boldsymbol{Q}]\{\ddot{\boldsymbol{p}}(t)\} + [\boldsymbol{D}]\{\dot{\boldsymbol{p}}(t)\} + [\boldsymbol{H}]\{\boldsymbol{p}(t)\} = \{\boldsymbol{q}(t)\} \quad (2)$$

where $[\boldsymbol{Q}]$, $[\boldsymbol{D}]$, $[\boldsymbol{H}]$, are the global acoustic inertia, damping and stiffness matrices, while $\boldsymbol{p}(t)$ is the column vector of the nodal pressure ($\{\boldsymbol{p}\} = -\rho\left\{\frac{\partial \Phi}{\partial t}\right\}$, with Φ the velocity potential function, ρ the fluid density) and $\boldsymbol{q}(t)$ is the column vector of nodal excitations generated by the volumetric sound sources into the cavity.

However, in order to model the response of a structural-acoustic coupled system, two additional terms must be added to equations (*1*) and (*2*) which take into account the acoustic-structural interaction. First, the transverse displacement of the plate produces volumetric acoustic excitation acting on the acoustic cavity, while the sound pressure represents the distributed force acting on the plate. So, considering the virtual work done by the plate displacement on the acoustic cavity and the virtual work done by the acoustic pressure on the plate, equations (*1*) and (*2*) can be written as

$$[\boldsymbol{M}]\{\ddot{\boldsymbol{w}}(t)\} + [\boldsymbol{C}]\{\dot{\boldsymbol{w}}(t)\} + [\boldsymbol{K}]\{\boldsymbol{w}(t)\} + [\boldsymbol{S}]\{\boldsymbol{p}(t)\} = \{\boldsymbol{f}(t)\} \quad (3)$$

$$[\boldsymbol{Q}]\{\ddot{\boldsymbol{p}}(t)\} + [\boldsymbol{D}]\{\dot{\boldsymbol{p}}(t)\} + [\boldsymbol{H}]\{\boldsymbol{p}(t)\} + [\boldsymbol{R}]\{\ddot{\boldsymbol{w}}(t)\} = \{\boldsymbol{q}(t)\} \quad (4)$$

where $[\boldsymbol{S}]$ is the global acoustic-structural coupling matrix, while $[\boldsymbol{R}]$ is the structural-acoustic coupling matrix. Since the reciprocity [23], the two coupling matrices are related such that $[\boldsymbol{S}] = [\boldsymbol{R}]^T$ and the dynamic response of the structural-acoustic coupled system can be described solving the system equations

$$\begin{bmatrix} [\boldsymbol{M}] & [\boldsymbol{0}] \\ -[\boldsymbol{S}]^T & [\boldsymbol{Q}] \end{bmatrix} \begin{Bmatrix} \{\ddot{\boldsymbol{w}}(t)\} \\ \{\ddot{\boldsymbol{p}}(t)\} \end{Bmatrix} + \begin{bmatrix} [\boldsymbol{C}] & [\boldsymbol{0}] \\ [\boldsymbol{0}] & [\boldsymbol{D}] \end{bmatrix} \begin{Bmatrix} \{\dot{\boldsymbol{w}}(t)\} \\ \{\dot{\boldsymbol{p}}(t)\} \end{Bmatrix} + \begin{bmatrix} [\boldsymbol{K}] & [\boldsymbol{S}] \\ [\boldsymbol{0}] & [\boldsymbol{H}] \end{bmatrix} \begin{Bmatrix} \{\boldsymbol{w}(t)\} \\ \{\boldsymbol{p}(t)\} \end{Bmatrix} = \begin{Bmatrix} \{\boldsymbol{f}(t)\} \\ \{\boldsymbol{q}(t)\} \end{Bmatrix} \quad (5)$$

Solving the system of equations (*5*), the pressure field due to the dynamic response of a structural-acoustic system when an external load excites the system, can be completely estimated.

3. Numerical Model

The developed numerical FE model includes two acoustic bodies upstream and downstream of the structural body, which represent the flexible plate. At the interface of the structural-acoustic bodies, fluid-structural boundary conditions are applied in order to define the system of equations described in equation (*5*). The downstream acoustic body is the air cavity enclosed, meanwhile the upstream acoustic body is included in order to apply an acoustic plane wave as the loading condition. In particular, an acoustic source is applied in the input plane of the upstream acoustic body, which is long enough so that a plane wave is fully developed before reaching the structural body. In the same input plane, radiation boundary conditions are applied, therefore acoustic waves normal to the boundary will be absorbed and not reflected back into the acoustic domain. Fixed structural boundary conditions are applied on the edges of the elastic plate in order to avoid any relative translational and rotational modes of the plate into the acoustic domain. Sound excitation was modelled as a plane wave from 100Hz to 800Hz, which yields a maximum and minimum wavelength of 1.37m and of 0.43m, respectively. Since the mesh should be fine enough to capture the acoustic and structural mode shapes, 6 elements per wavelength were used according to the high frequency.

An example of the FE model is shown in Figure 1.

Harmonic analysis is set on the frequency range of interest (100Hz - 800Hz) and equation (5) is solved estimating the pressure field of the acoustic bodies and the displacement-velocity of the structural elements. In order to characterize the acoustic performance of the acoustic resonator, the Transfer Function Method (24-25-26) is applied. When the pressure field is completely estimated in the upstream acoustic body, the sound pressures (p_1 and p_2) (equation (*5*)) at two microphone locations can be acquired, where the spacing between the two microphones (s) is defined to be less than 80% of shortest half wave length of interest (24) ($s < 0.4\frac{c}{f_u}$, with f_u is the upper frequency in the frequency range of interest). The reflection coefficient (*R*) is expressed through the transfer function between the complex pressures measured at two microphone positions ($H_{12} = \frac{fft(p_2)}{fft(p_1)}$) and the transfer function of the incident (H_i) and the reflecting (H_r) plane sound wave

$$R = \frac{H_{12} - H_i}{H_r - H_{12}} e^{[2jk_0(L+s)]} \quad (6)$$

where *s* is the microphones spacing, *L* is the distance between the plate of the acoustic resonator and the closer microphone location and k_0 is wave number. The transfer function of the incident and reflecting sound waves at the two microphone locations are expressed as

$$H_i = e^{(jk_0 s)} \quad (7)$$

$$H_r = e^{-(jk_0 s)} \quad (8)$$

So the sound absorption coefficient of the acoustic resonator can be the estimated by [29]

$$\alpha = 1 - |R| \quad (9)$$

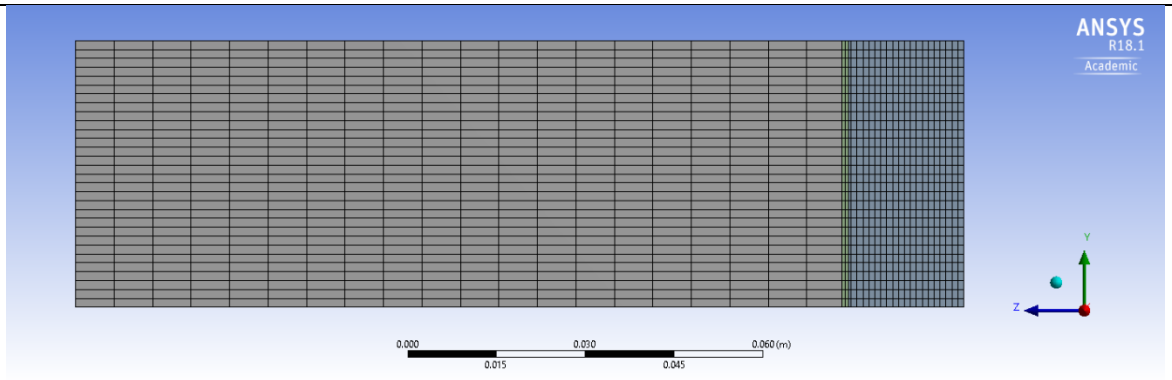

Figure 1. FE model the acoustic resonator for the acoustic performance evaluation

3.1. Parametric Analysis

The proposed membrane-type unit cell includes a square elastic plate (45x45mm) of certain thickness (*t*) with an enclosed cavity of certain depth (*D*).

The proposed numerical FE model is used to perform a parametric analysis in order to understand the effect of the geometrical parameters of the resonator (*t, D*) and the material properties of the membrane (*ρ, E*) on the absorption performance of the resonator.

The effect of the plate thickness is studied in a frequency range between 100-800Hz keeping constant the cavity depth (*D* = 20mm), the plate size (45x45mm) and the material properties (*E* = 1.65MPa and ρ = 1200 Kg/m^3).

The effect of the plate resonator thickness on the sound absorption is shown in Figure 2.

For thin membrane (t = 0.5mm), the resonator behaves as a common membrane-type resonator showing a single high peak in the absorption coefficient. Small thickness variations induce considerable changes in the absorption properties. Increasing the membrane thickness the frequency range where the maximum resonator absorption properties may be noticed is shifting at lower frequencies. However the absorption frequency range is not the only parameter which is affected by the membrane thickness. For membrane of thickness between 1 and 2 mm, the normal absorption coefficient shows not 1 peaks anymore, but two considerable peaks close in frequency. Further increasing the thickness, the two absorption peaks start to move away to each other and the absorption of the second peak starts to reduce in amplitude, until only the first peak becomes relevant.

The effect of the membrane thickness can be summarized as follow. Increasing such parameter a main shift at lower frequencies can be observed for the absorption working frequency range, and three limit cases can be identified. For thin membrane (t=0. 5mm) only one absorption peak is relevant at high frequencies, for thicker membranes (t=3.0mm) only one peaks is dominant at lower frequencies, while for intermediated values 1.0mm<t< 2mm) two absorption peaks can be observed very close in frequencies which provide a quite broadband absorption.

After evaluating the effects of the membrane thickness, the effect of cavity depth is investigated for a membrane of 1.2mm thickness (size of 45x45mm, *E* = 1.65MPa and ρ = 1200 Kg/m^3), since this thickness provide a double peak and broadband absorption. Increasing the depth of the enclosed cavity, the absorption peaks are shifting at lower frequencies on average (Figure 3). Also in this case three main cases can be identified. For high values of cavity depth (D=40mm) the absorption is dominated by the first peak at lower frequency, while there is drop in amplitude of the second peaks. On the other hand, the second absorption peak at higher frequencies is dominant with small cavity depth (D=15mm). Resonators with cavity depth around 20mm keep the double peak and guarantee a broadband absorption.

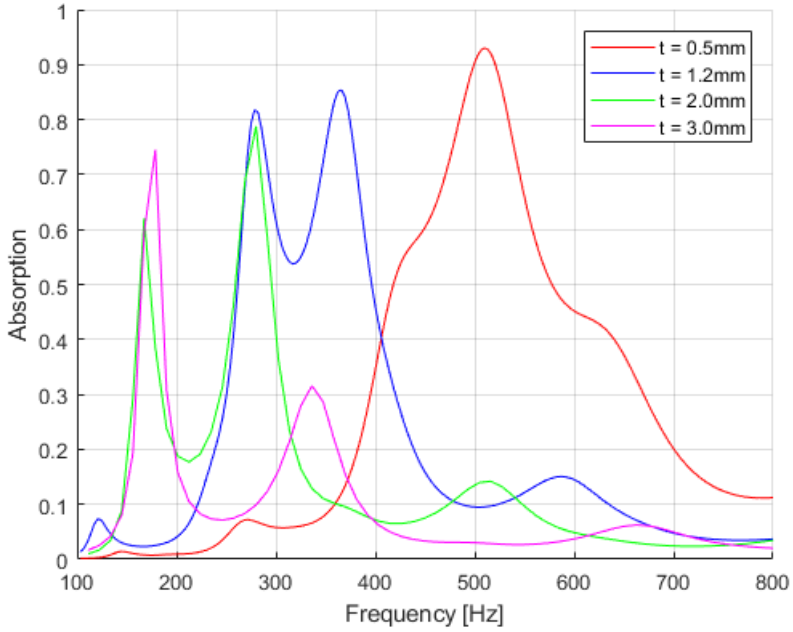

Figure 2. Parametric study of the resonator absorption coefficient varying the plate thickness (E = 1.65MPa and ρ = 1200 Kg/m3, d = 20mm)

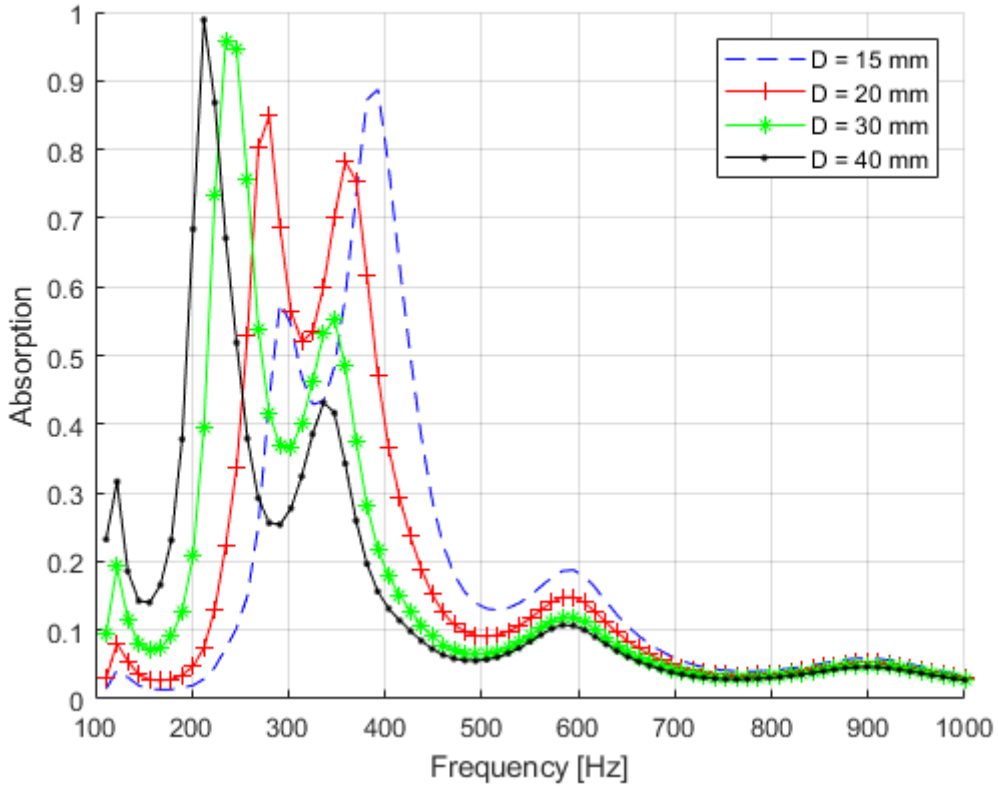

Figure 3. Parametric study of the resonator absorption coefficient varying the cavity depth (E = 1.65MPa and ρ = 1200 Kg/m3, t = 1.2mm)

At this stage, the plate material properties effect on the sound absorption is investigated, keeping constant the geometrical parameters (*t = 1.2mm, D=20mm*).
The material density doesn't affect the global shape of the absorption profile, but increasing the density of the resonator plate, the absorption coefficient peaks shift at lower frequencies with a reduction of the absorption level (Figure 4). In particular increasing the density from 500 Kg/m^3 to 2000 Kg/m^3 the main absorption peak move from 430 Hz to 210 Hz with a drop in amplitude of 15%.
When the density increases the out of plane membrane displacement will be lower when excited by a plane sound wave. It means the absorption level will be lower because less sound energy will be dissipated through the resonators vibration.
Not only the materials density plays a key role on the sound absorption of the acoustic resonator. As long as the ration *E/ρ* is kept constant, the acoustic properties of the resonator do not change, in the other cases, the effect of the *E/ρ* will affect the acoustic absorption of the resonator.
Figure 5 shows the parametric analysis of the sound absorption coefficient with different values of *E/ρ*, while keeping the resonator geometrical parameters constant (*t = 1.2mm, D=20mm*). An optimal value of *E/ρ* = 1.4e3 m^2/s^2 can be identified where the resonator shows a broadband absorption between 240 Hz -400 Hz with a sound absorption level all over 50% and two different peaks at 268 Hz and 369 Hz with 82% and 85% absorption. Moreover *E/ρ* = 1.0e5 m^2/s^2 represents a limit value which results in only a single absorption peak

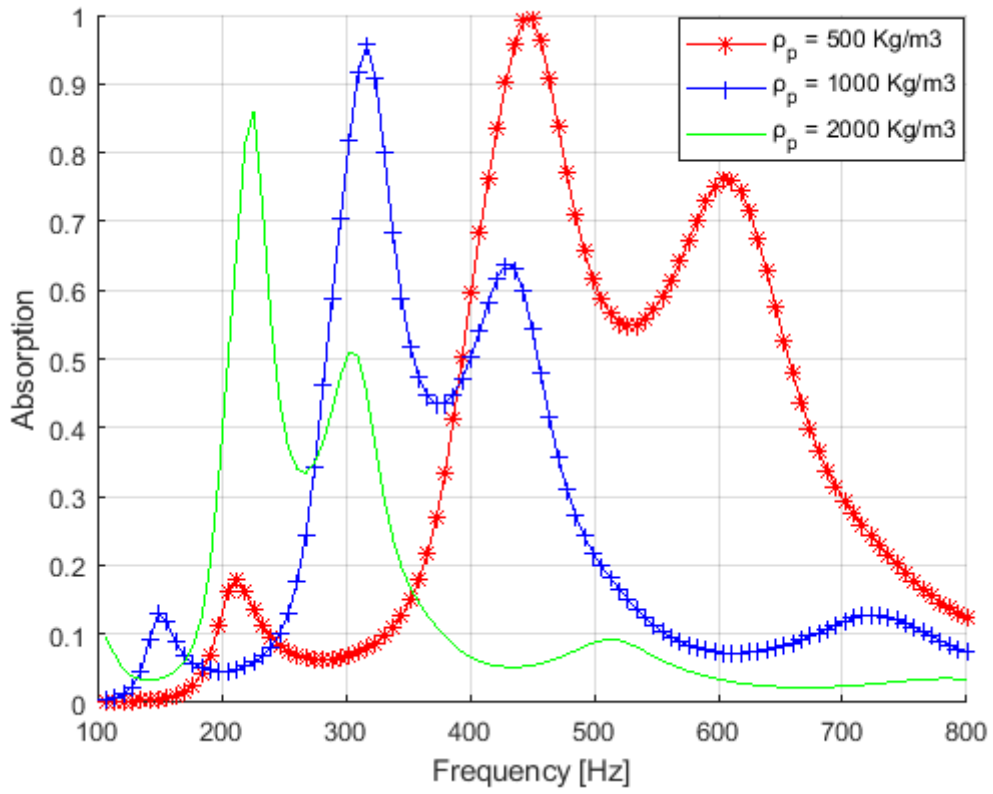

Figure 4. The absorption coefficient of the resonator absorber varying with the plate density (45x45mm plate, t = 1.2mm, D=20mm, E=1.9MPa)

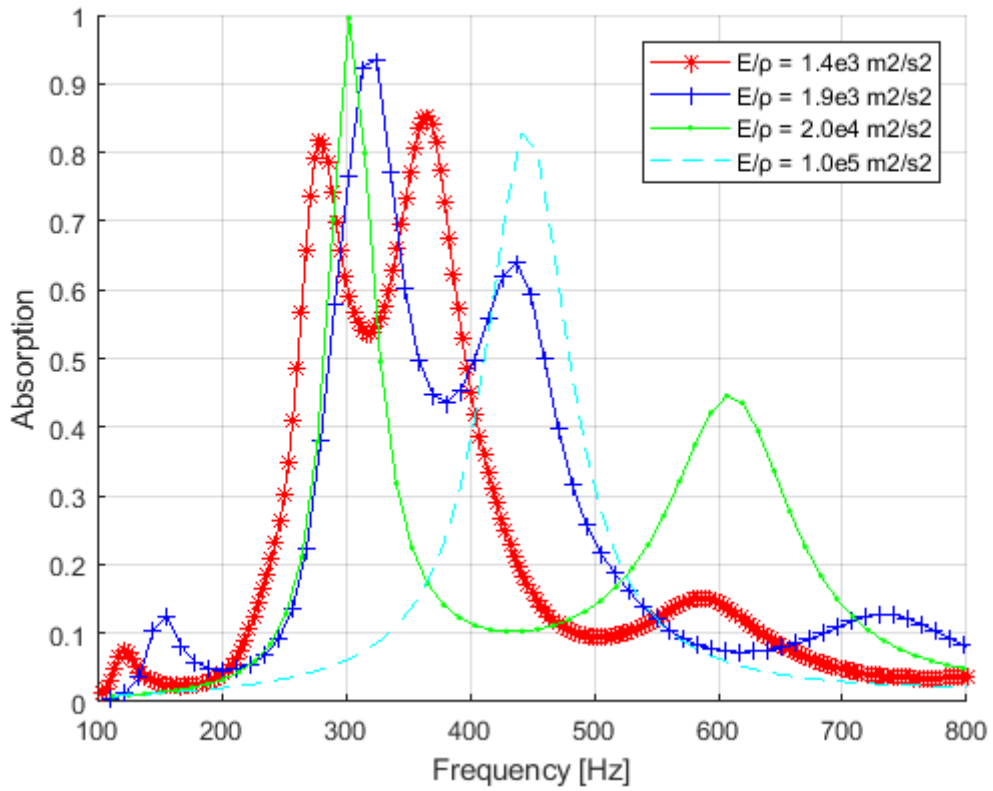

Figure 5. The absorption coefficient of the resonator absorber varying with the ratio E/ρ (45x45mm plate, t = 1.2mm, D=20mm)

3.2. Numerical Model Validation

The parametric analysis results are used to identify the optimized configuration for the resonator. This optimum configuration is chosen to validate the proposed FE numerical model.

The resonator unit cell is machined and tested in an impedance tube test ring in order to measure the normal sound absorption which will be compared with the numerical one.

The considered acoustic resonator unit cell (Figure 6) consists of a square elastic plate (45x45mm) of 1.2mm thickness with an enclosed cavity of 22mm depth. The plate is made of silicone by casting process and the elastic properties of the material is measured through tensile testing. According with ISO 527 – 1:1996 (27) dog bone shape samples are tested with a test speed of 1 mm/min and the stress-strain curve is shown in Figure 6. The Silicone shows an elastic modulus of 1.65MPa and a density of 1200 Kg/m^3.

The material is tested also through Dynamic Mechanical Analysis (DMA) in order to measure the damping properties of the used silicone. DMA results show a constant trend of the tanδ over the frequency which can give us an indication about the damping coefficient (tanδ$\approx 2\xi$ [30-31]). From such result a constant structural damping of 0.1 is applied on the material properties definition of the FE model.

These experimental results are used as input data in the numerical simulation.

The unit cell is tested in a two microphones impedance tube test rig, according with the ASTM E 1050 (24), for which the working frequency range (interval where plane-standing wave conditions are guaranteed) is 250-3000 Hz. However at this stage, the normal incident sound absorption coefficient is measured in a sub-frequency range between the 250Hz to 800 Hz in order to validate the numerical results.

The measured and numerical sound absorption coefficient are plotted in Figure 7 which shows a good agreement between the experimental and numerical result, and small differences in terms of amplitude is due to the assumption of a constant damping ratio in the numerical model.
In conclusion, the proposed FE numerical model is a usefulness approach to predict the acoustic properties of the proposed membrane-type acoustic resonator and can be used to better understand the absorption mechanism. Moreover, the experimental measurement demonstrates that the proposed unit cell acoustic resonator provides subwavelength absorption with two considerable absorption peaks at 268 Hz and 369 Hz. Unlike usual membrane-type metamaterial or resonator absorbers, the absorption performances of the proposed resonator is not identified by a single narrow peak. Optimizing the physical properties of the resonator, in terms of geometry and material properties, a double absorption peak is generated broadening the frequency range in which the sound absorption is considerable high (over 50%).

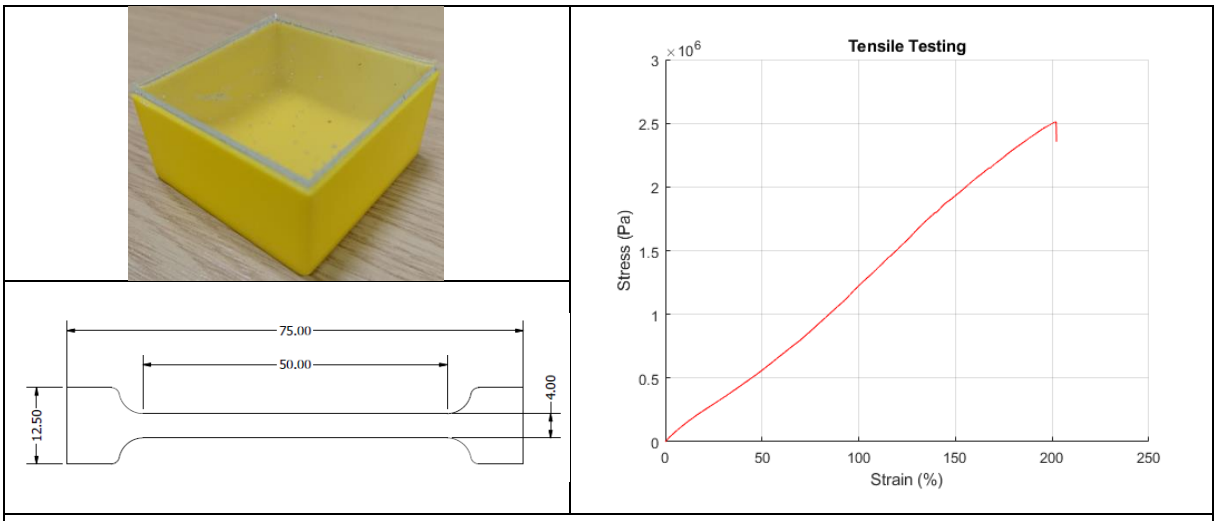

Figure 6. (Left-Up) Acoustic resonator unit cell; (Left-Bottom) Dog bone shape sample for tensile testing; (Right) Stress-Strain curve for Silicone measured by tensile testing

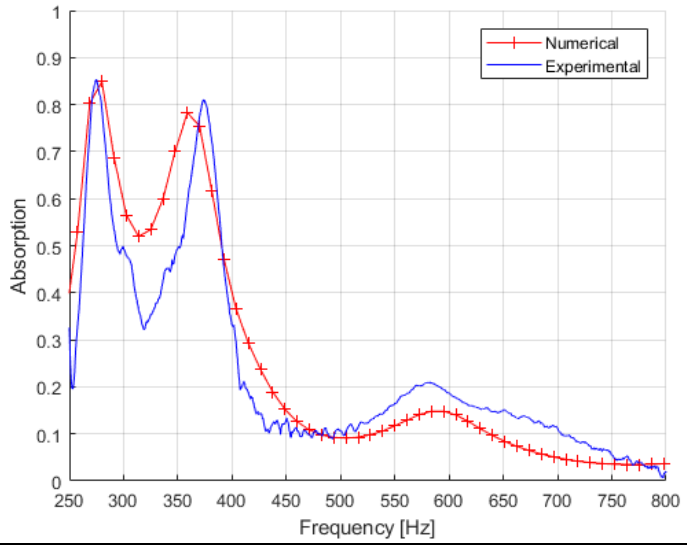

Figure 7. Comparison between the experimental sound absorption coefficient (blue line) and the numerical one (red line) estimated with FE model

4. Results and Discussion

In this section the validated numerical model is used to better understand the absorption mechanism of the proposed resonator.

The optimized unit cell resonator shows an extended low frequency response in the sound absorption coefficient which is characterized by two main absorption peaks. In this section the optimized unit cell acoustic performances are compared with a non-optimized one in order to study the reasons behind such broadband and mutli-peaks absorption which is unusual for a membrane-type metamaterial.

In particular, keeping constant the material properties (elastic modulus of 1.65MPa and a density of 1200 Kg/m^3), the unit cell size (45x45mm) and the enclosed cavity depth (D=22mm), two membrane thickness are investigated: the optimized t=1.2mm and the non-optimized t=0.5mm one.

In order to investigate the actual acoustic-structural interaction for the unit cell resonator when it is excited by an acoustic sound wave, the acoustic response of the enclosed cavity and the structural response of the membrane of the two considered case studies are deeply analysed further in this section. The acoustic response of the resonator is studied in terms of difference (Δp) between the pressure into the unit cell chamber and the upstream sound pressure (Figure 9), while the structural response is expressed in terms of Frequency Response Function (*FRF*) estimated using the out of plane velocity response of the resonator membrane (Figure 10).

The Δp and the *FRF* are estimated according with the proposed FE modal in a frequency range between 100Hz and 800Hz.

The two case studies are discussed individually below.

4.1. Non-optimized unit cell resonator (t=0.5mm)

The absorption coefficient (Figure 8 (a)) for the unit cell resonator with a membrane of 0.5mm thickness presents only one peak at 513 Hz.

First of all the membrane structural dynamic response is discussed.

Taking into account the structural response of the membrane described by the FRF, as well-known at that frequency where the membrane presents a structural resonance the FRF show a peak in modulus, a phase shifting, a relative maximum/minimum in the imaginary part zero value in the real part.

In this case of membrane with 0.5mm thickness, it clear that the membrane presents a structural resonance at 515 Hz (Figure 10– Red line). To confirm such result extracted from the FRF, a modal analysis is performed on a fixed-supported membrane with the same geometry and material properties of the unit cell resonator membrane. The modal analysis demonstrate that a symmetric bending mode appears at the resonance frequency of 515Hz (Figure 8 (b)). Comparing now the structural response of the membrane itself with the unit cell resonator acoustic performances, we can notice a perfect match between the structural resonance frequency (515 Hz) and the absorption peak (513 Hz), which suggests that the absorption mechanism is related to the sound energy dissipation due to the resonance phenomena of the membrane resonator.

Consider now the acoustic response.

According with the general formulation of the acoustic resonator which could be the membrane type resonator, the acoustic resonance frequency is related to the mass density per unit area of the membrane (m) and the cavity depth (d) [28]

$$f_r = \frac{c}{2\pi}\sqrt{\frac{\rho}{md}} \quad (10)$$

where c is the sound speed in air and ρ is the air density. Applying this formula to the unit cell resonator, the acoustic resonance can be identified at at 516 Hz, which is basically the acoustic resonance of the resonator chamber. There is perfect match in frequency between the structural resonance (515 Hz) of the plate and the acoustic resonance of the chamber (516Hz). So the sound absorption is not only related to the structural resonance of the membrane itself but it is rather due

to resonance of the global resonator. In other words, the mass of the plate is being treated as single lump mass and therefore the plate should vibrate as a piston and the effect of the cavity is only a lump stiffness of the system.

The Δp between the chamber pressure and incoming sound pressure and the isosurface for the pressure distribution in the chamber and in the upstream acoustic body are used to support that thesis.

From the real part of the Δp plotted in Figure 9 – red line, a positive peak is picked up at the max absorption frequency, which means that a such frequency the air mass into the resonator chamber is moving in-phase with the sound wave excitation.

In Figure 8 (c-d) the isosurface are plotted. For each section the pressure, both into the resonator chamber and in the upstream acoustic body, is constant. Moreover, focusing on the isosurface at the upstream and downstream membrane interface, we can see how a constant pressure distribution is distributed at upstream and downstream membrane interface. The small proximity pressure changing at the downstream interface are due to the membrane resonance at that frequency, however these changing are ±2% around the mean pressure value on average. So we can assume constant pressure distribution. Also the constant pressure distribution upstream and downstream the membrane present the same sign which confirm that the membrane-chamber system is vibrating as a single degree of freedom piston.

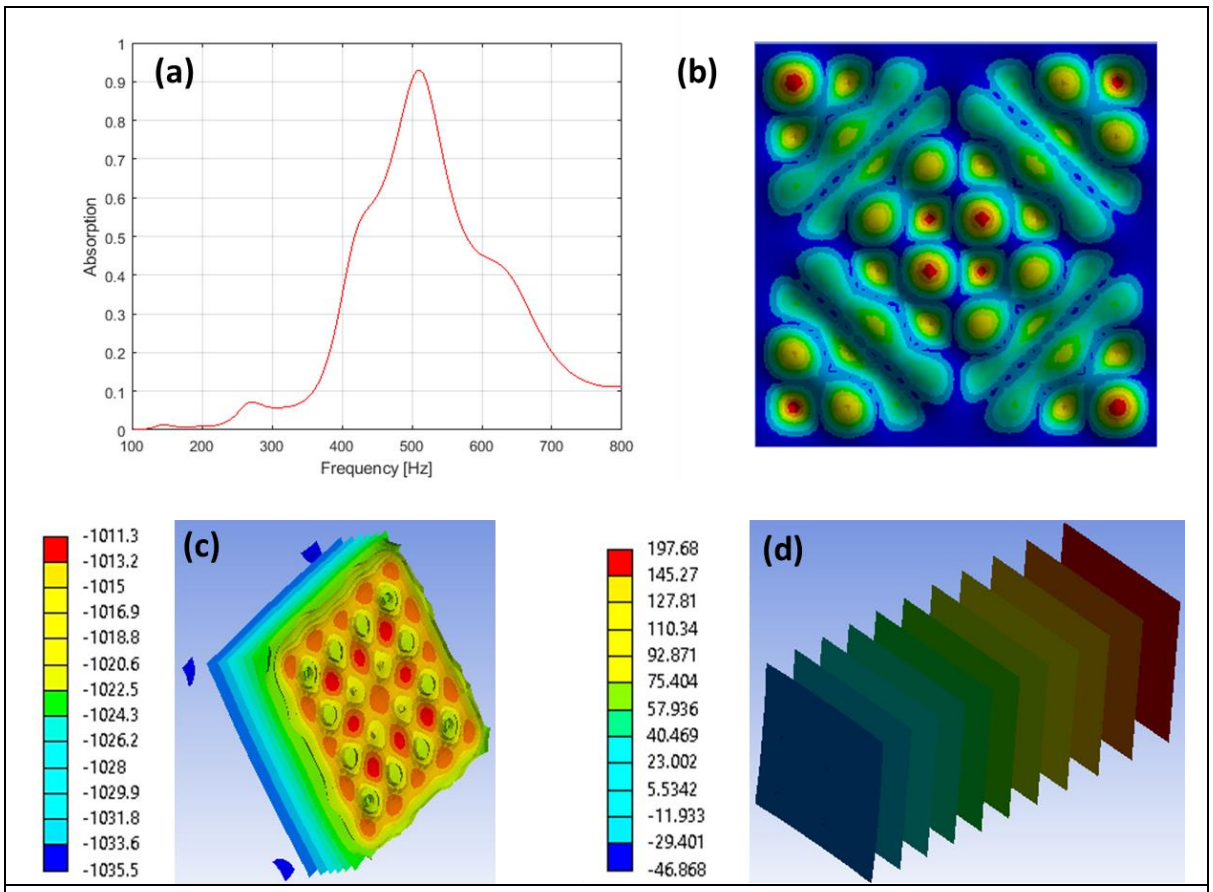

Figure 8. Unit cell resonator t=0.5mm (45x45mm, D = 22mm, E = 1.65MPa and ρ = 1200 Kg/m3): (a) Absorption coefficient; (b) Modal Analysis: membrane mode shape at 515Hz; (c) Isosurface downstream the membrane; (d) Isosurface upstream the membrane.

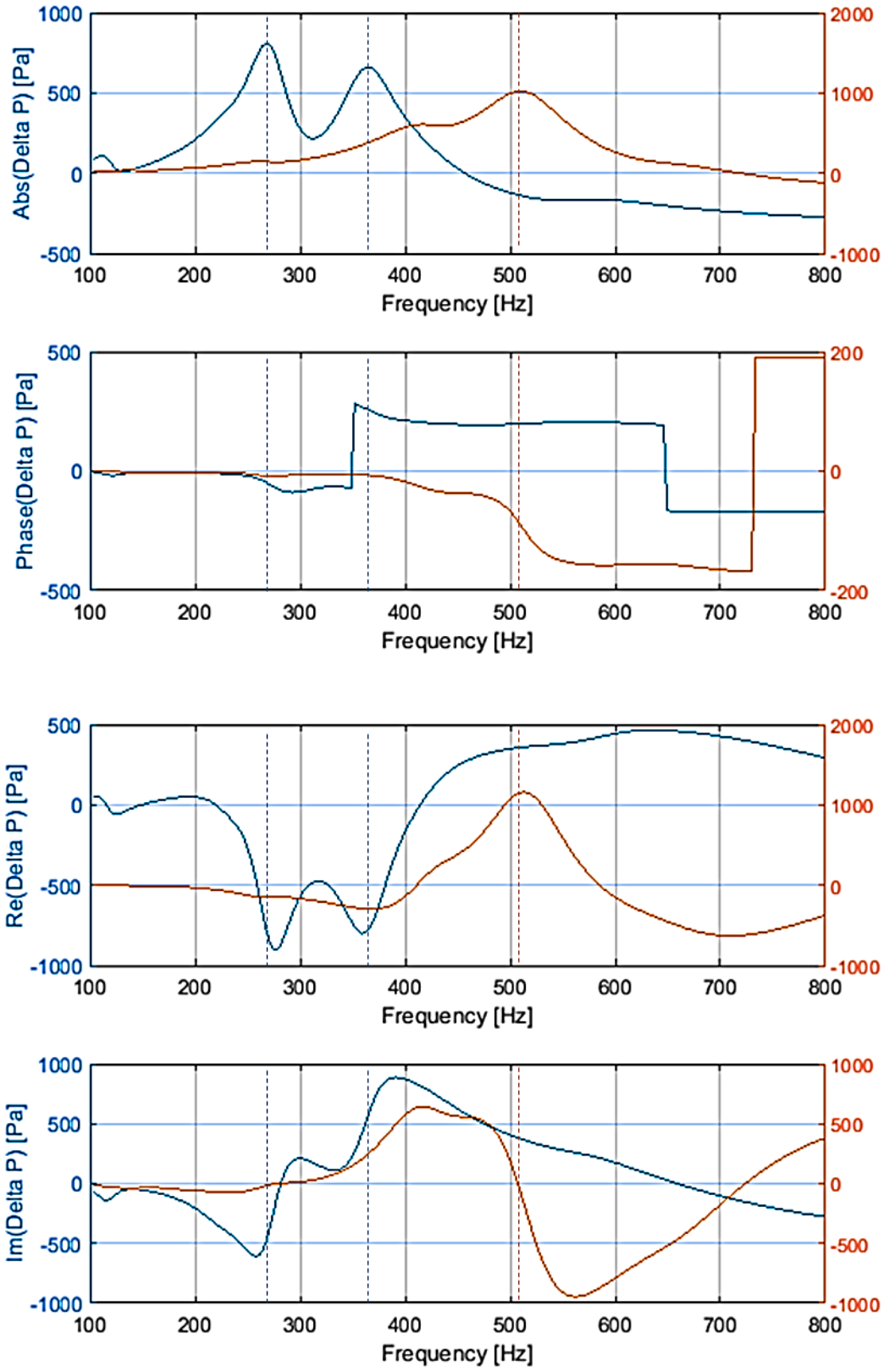

Figure 9. Modulus and Phase (upper plots) and Real and Imaginary part (lower plots): resonator with 1.2mm membrane thickness – Blue line; resonator with 0.5mm membrane thickness – Red line.

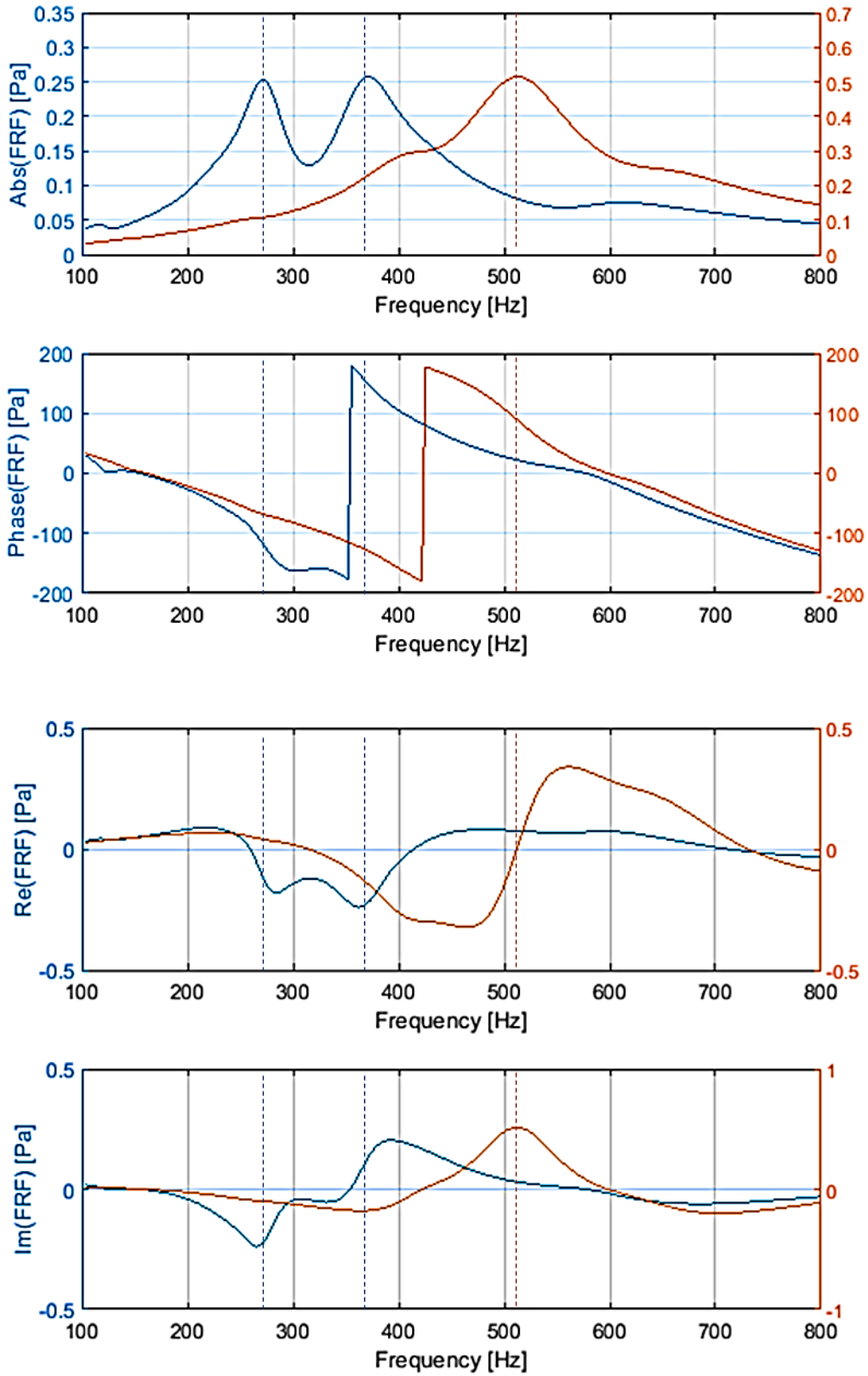

Figure 10. Modulus-Phase (upper plots) and Real-Imaginary Part (lower plots) of Velocity Frequency Response Function: resonator with 1.2mm membrane thickness – Blue line; resonator with 0.5mm membrane thickness – Red line.

4.2. Optimized unit cell resonator (t=1.2mm)

The absorption coefficient (Figure 11(a)) for the optimized unit cell resonator (membrane of 1.2mm thickness) presents two peaks at 268 Hz and 369 Hz.

As we discuss for the non-optimized unit cell resonator, first of all we take into account the structural response of the only membrane when it is excited by an acoustic sound wave.

As we describe above for the non-optimized resonator, the FRF measured on the membrane give us an indication about the structural resonance frequency of the membrane itself.

The FRF for the optimized membrane is plotted (Modulus-Phase and Real-Imaginary Part) in Figure 9 – Blue line. In this case, the FRF show peaks in the modulus and a phase changing at the maximum absorption frequencies: 268Hz and 369 Hz. However, at these frequencies the real part is not zero and the relative maximum/minimum in the imaginary part which is usually associated to a structural resonance, are shifted at different frequencies with respect to the absorption peak frequencies.

Also in this case, we run a numerical modal analysis on an equivalent membrane applying the equivalent boundary conditions, to verify the actual structural resonance frequencies and the relative mode shapes. Since a plane wave can excite only the symmetric bending modes of the membrane, only these mode has been taken into account from the modal analysis in the frequency range of interest (100Hz-800 Hz). Three main structural resonance frequencies are picked up in that frequency range respectively at 231 Hz, 323 Hz and 406 Hz , and the relative mode shapes are plotted in Figure 11 (b1-2-3), which are close to the absorption peak frequencies but don't match them. In other words the absorption peaks in this case is not associated to pure structural resonances of the resonator membrane.

If we consider now the acoustic response contribution, according with equation *(10)* an acoustic resonance can be identified at 356 Hz which is in between the absorption peaks frequencies. So the absorption mechanism behind the optimized resonator is not strictly related to the structural resonance of the membrane and it is not even strictly related to the acoustic resonance of the air into the enclosed cavity. Moreover, while the numerical model presented by equation *(10)* leads to an acoustic resonance of 356 H, the resonator does not behave like a single degree of freedom piston which is instead the main reason behind the single absorption peak of the commonly used membrane-type metamaterial.

In Figure 9 – Blue line, we plot the upstream-downstream Δp for the optimized resonator. Focusing on the real part, we can see how at the absorption peak frequencies the real part of Δp shows two negative peaks which means that the air mass into the resonator chamber is moving out of phase with the incoming sound wave excitation. In other word, on the contrary to the non-optimized unit cell resonator, the enclosed air mass react out of phase with the incoming sound wave which excite the unit cell resonator. This is confirmed by the pressure isorsurface plotted in Figure 11 (d1-2) respectively for the maximum absorption frequencies (268Hz and 369 Hz). For both the frequencies 268Hz and 369Hz, the mean value of the incoming pressure wave is positive while mean value of the reaction pressure in the enclosed cavity is negative, so the pressure field of the incoming pressure wave and the resonator's chamber are opposite in sign. Looking at the isosurface at upstream and downstream interface of the membrane, the pressure distribution at the interface is not constant which means that the resonator is not behave as a piston. Moreover the isosurface in the chamber show how the higher acoustic modes of the mass air in the chamber are excited at the absorption peak frequencies. The non-uniform pressure distribution due to higher acoustic modes of the chamber will act on the membrane which, on the other hand will react according with its intrinsic mode shapes related to its structural resonances excited by the incoming sound wave excitation. This interaction between the higher acoustic modes and structural modes generated a hybrid resonances of the resonator assembly which dissipate the sound energy associated to the incoming sound wave.

So for the optimized resonator, the high absorption is still related to sound energy dissipation resonance phenomena of the resonator, but in this case the resonance are not pure structural membrane resonance or pure acoustic resonance of the enclosed cavity. The mutual interaction of structural dynamic of the membrane and the acoustic dynamic response of the air into the cavity must

be taken into account as a combination of the higher structural and acoustic modes. As a consequence, the maximum absorption, is related to the hybrid resonances of the coupled structural-acoustic system due to non-uniformly distributed pressure acting on the membrane, which is not behave as piston anymore.

The proposed optimized resonator is designed to move close the structural-acoustic hybrid resonances in order to broaden the absorption at low frequencies.

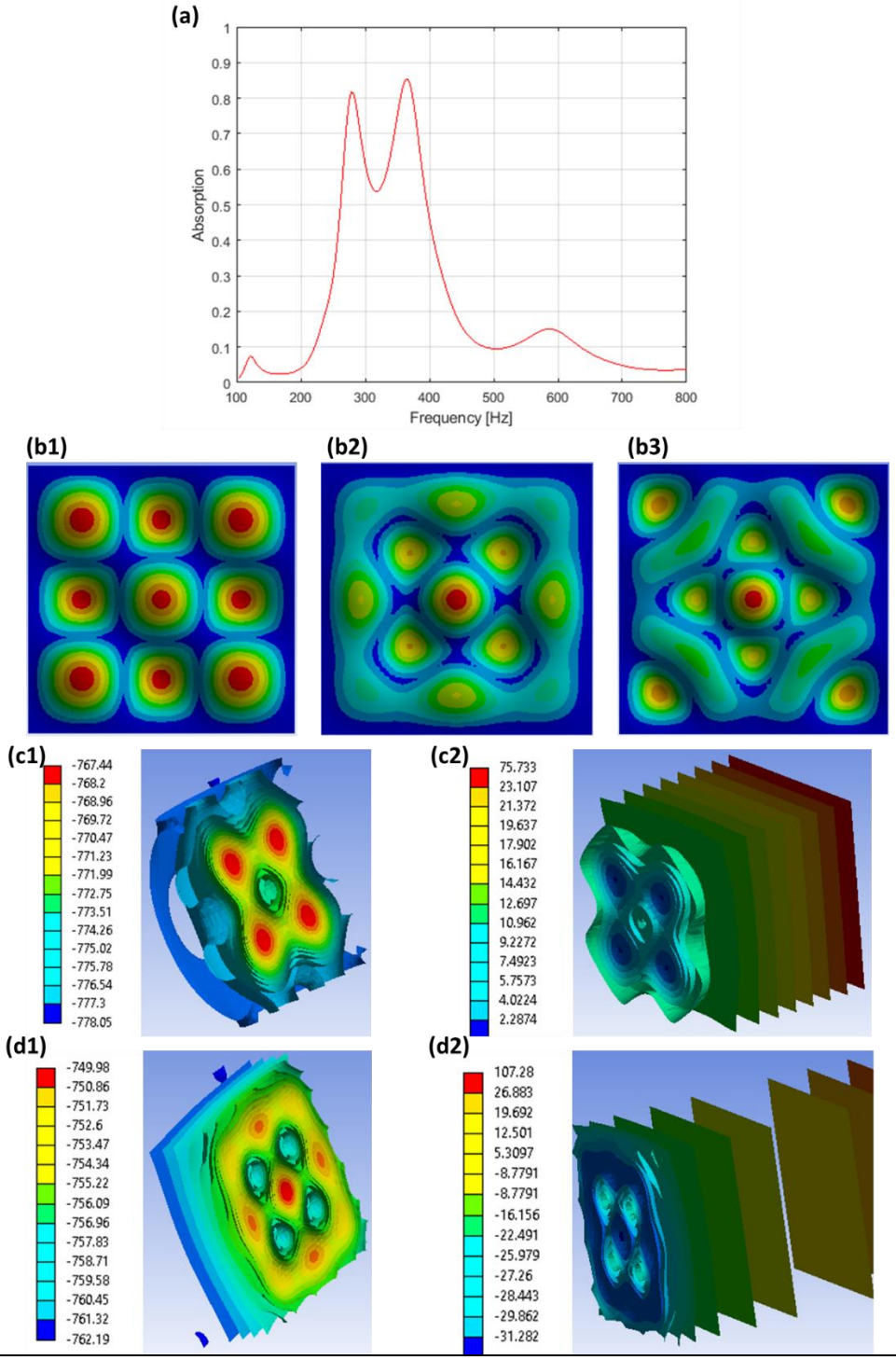

Figure 11. Unit cell resonator t=1.2mm (45x45mm, D = 22mm, E = 1.65MPa and ρ = 1200 Kg/m3): (a) Absorption coefficient; (b) Modal Analysis: membrane mode shape at 231 Hz (b1), 323 Hz (b2) and 406 Hz (b3); (c) Isosurface downstream (c1)-upstream (c2) the membrane at268 Hz ; (d) Isosurface downstream (d1)-upstream (d2) the membrane at 369Hz.

4.3. Effect of the geometrical parameters and material properties on the absorption

Now that absorption mechanism of the proposed membrane type unit cell has been deeply discussed and the reasons behind the improvement of the absorption properties with respect to the common membrane type resonator has been demonstrated, it is easy to understand the effect of the geometrical parameters which are presented in previous parametric analysis.

Considering first of all the membrane thickness effect (Figure 2).
Changing the thickness of the membrane, the entity of the interaction between the structural dynamic response and the acoustic response of the resonator will change as consequence. For small thickness the structural dynamic response of the membrane does not have a great effect. In this case the effect of the membrane is a lump mass which reacts in phase with the mass air in the enclose cavity where the higher acoustic modes are not excited. So the structural-acoustic interaction can be described as a single degree of freedom mass spring system. Increasing the thickness of the plate, the vibration of the plate itself will be not neglectable. Moreover the mutual interaction between the membrane and enclose air mass lead to a non-uniform upstream-downstream pressure with consequent excitation of the higher acoustic modes in the chamber. Hybrid structure-acoustic resonance come out due to the coupling of higher structural modes of the plate and acoustic modes of the chamber; thus leading to multiple absorption peaks.

The main effect of the cavity depth is on the acoustic response of the unit cell.
Considering the simple case of piston behaviour (single degree of freedom) of the unit cell, the acoustic resonance of the enclosed cavity is described by equation *(10)*. According with such equation, increasing the depth, the acoustic resonance moves towards lower frequencies.
Considering now the optimized unit cell which provides multiple absorption peaks, the cavity depth changing will affect the mutual acoustic-structural interaction. In particular, since the acoustic cavity mode moves towards lower frequencies (according to equation *(10)*) as the cavity depth is increased, the coupling with the structural modes will change and will be stronger at lower frequencies for bigger cavity depth. So for bigger cavity depth, the sound absorption (Figure 3) will be dominated by the coupling between the acoustic modes shifted at lower frequencies and the relative structural modes at lower frequencies; while reducing the cavity depth the acoustic modes will move at higher frequencies and they will couple with the structural modes at higher frequencies increasing the global absorption performance of the unit cell resonator at higher frequencies.

The material density for the resonator membrane affects both the structural dynamic response of the membrane and the acoustic one of the cavity. Both the acoustic resonance (equation *(10)*) and the structural resonance are inversely proportional ($\sim 1/\rho_p$) to the material density, so hybrid structural-acoustic resonances at lower frequencies of the acoustic resonator can be expected because of density increases. Considering the optimized unit cell resonator, the main effect of the density increasing is the translation of the absorption peaks at lower frequencies. However, when density increases the response displacement of the membrane will be lower when excited by an incoming sound wave. It means the absorption level will be lower because less sound energy will be dissipated through the resonators vibration.
More than the material density, the ratio E/ρ plays a key role on the sound absorption of the proposed acoustic resonator. As long as the ration E/ρ is kept constant, the acoustic properties of the resonator do not change, in the other cases, the effect of the E/ρ will affect the acoustic-structure interaction between the resonator plate and the resonator chamber as well as we discussed for the membrane thickness variations. In particular the proposed resonator presents an optimal value of E/ρ = 1.4e3 m^2/s^2 where the structural-acoustic coupling results in broadband absorption between 240 Hz -400 Hz with a sound absorption level all over 50% and two different peaks at 268 Hz and 369 Hz with 82% and 85% absorption. Increasing the ratio results in a reduction in the hybrid resonances due to structural acoustic interaction. A limiting value of E/ρ = 1.0e5 m^2/s^2 was determined, which results in only a

single absorption peak due to the plate vibrating as a piston and thus the effect of the cavity is only a lump stiffness of the system.

5. Conclusions

Membrane-type metamaterials provide good sound absorption at low-frequencies, however wide band absorption is difficult to achieve in one device, as they are categorised by a single narrow absorption peak. Therefore, the frequent challenges in the design of membrane-type and resonator absorbers is to extend the frequency bandwidth. A subwavelength acoustic resonator unit cell was proposed in this paper which included an elastic silicone plate of 1.2mm thickness with an enclosed air cavity of 22mm depth. The results showed that it was possible to achieve two high and broadening absorption peaks over 80% at 268Hz and 369Hz, which provided broadband absorption in the frequency range between 250Hz and 400Hz. Using an acoustic-structural interaction based numerical model, it was demonstrated that the absorption of the resonator was associated to hybrid resonances which occur when high order structural modes of the elastic plate are coupled with the acoustic modes of the cavity. Furthermore, the sound absorption performance is related to the geometry and material (inertia and elastic properties) characteristics of the resonator absorber. Thus, it was shown that by optimisation of these parameters, the membrane absorber can be tuned to achieve the best performances in the specified frequency range using very cheap materials.

6. References

1. Yang M., Sheng P., Sound Absorption Structures: from porous media to acoustic metamaterials, Annual Review of Material Research, Vol 47:83-114 (2017).
2. Maa D.Y., Theory and design of microperforated panel sound absorbing construction, Sci Sin, 18:55-71 (1975).
3. Maa D. Y., Potential of microperforated panel absorber, Journal Acoust Soc A, 29:77-84 (1987).
4. Wang C., Huang L., On the acoustic properties of parallel arrangement of multiple micro-perforated panel absorbers with different cavity depths, Journal Acoust. Soc. Am, Vol.130, No1, (2011).
5. Guo W., Min H., A compound micro-perforated panel sound absorber with partitioned cavities of different depths, IBPC, 78: 1617-1622, (2015).
6. Bucciarelli F., Malfiense F., Meo M., A multilayer microperforated panel prototype for broadband sound absorption at low frequencies, Applied Acoustics, 146: 134-144 (2019).
7. Pan J., Guo J., Ayres C., Improvement of Sound Absorption of Honeycomb panels, Proceeding of Acoustics 2005.
8. Sakagami K., Yamashita I., Yairi M., Morimoto M., Effect of honeycomb on the absorption characteristics of double-leaf microperforated panel (MPP) space sound absorbers, Noise Control Eng. J. 59.4:363 (2011).
9. Sakagami K., Fukutani Y., Yairi, Morimoto M., Sound absorption characteristics of double-leaf structure with an MPP and a permeable membrane, Applied Acoustics, 76: 28-34, (2014).
10. Sakagami K., Morimoto M., Yairi M., A note on the relationship between the sound absorption by microperforated panels and panel/membrane type absorbers, Applied Acoustics, 70: 1131-1136, (2009).

11. Ma G., Sheng P., Acoustic metamaterial: From local resonators to broad horizons, Sci. Adv. 2(2), el1501595 (2006).
12. Huang T.-Y., Shen C., Jing Y., Membrane-and plate-type acoustic metamaterials, J. Acoust. Soc. Am., 139 (6) (2016).
13. Yang Z., Mei J., Yang M., Chan N. H., Sheng P., Membrane-type acoustic metamaterial with negative dynamic mass, Phys. Rev. Lett. 101(20), 204301 (2008).
14. Naify C. J., Chang C. M., McKnight G., Nutt S., Transmission Loss and dynamic response of membrane-type locally resonant acoustic metamaterial, J. Appl., Phys. 108 (11), 114905 (2010).
15. Naify C. J., Chang C. M., McKnight G., Nutt S., Transmission loss of multi-celled arrays, J. Appl. Phys., 109(10), 104902 (2011).
16. Mei J., Ma G., Yang M., Yang Z., Wen W., Sheng P., Dark acoustic metamaterials as super absorber for low-frequency sound, Nat. Commun. 3, 756 (2012).
17. Ma G., Yang M., Xiao S., Yang Z., Sheng P., Acoustic metasurface with hybrid resonances, Nat. Matt. 3:873-878 (2014).
18. Yang M., Ma G., Yang Z., Sheng P., Coupled membranes with doubly negative mass density and bulk modulus, Phys. Rev. Lett. 110(13), 134301 (2013).
19. Zienkiewicz O. C., Taylor R. L., The finite element method for solid and structural mechanics, Butterworth-Heinemann (2013).
20. Petyt M., Introduction to finite element vibration analysis, Cambridge University Press (2010).
21. Reddy J. N., Mechanics of laminated composite plates and shells, CRC (2004).
22. Glandwell G.M.I., Zimmermann G., On energy and complementary energy formulations of acoustic and structural vibration problems, J. Sound Vib., 1996.
23. Fahy F., Gardonio P., Sound and structural vibration: Radiation, Transmission and Response, Technology & Industrial Arts 1985.
24. ASTM E 1050, Standard test method for impedance and absorption of acoustical materials using a tube, two microphones and a digital frequency analysis system, ASTM INTERNATIONAL (2012).
25. Seybert A. F., Ross D. F., Experimental determination of acoustic properties using a two-microphone random-excitation technique, J. Acoust. Soc. Am. 61, 1362-1370 (1977).
26. Chu W. T., Extension of two-microphone transfer function method for impedance tube measurement, J. Acoust. Soc. Am. 80, 347 (1986).
27. ISO 527 – 1 : 1996, Plastic – Determination of tensile properties, British Standard Institution (1996).
28. Cox T. J., D' Antonio P., Acoustic Absorption and Diffusers: Theory, Design and Application, Spon Press (2004).
29. D.T. Blackstock, Fundamentals of Physical Acoustics, JOHN WILEY & SONS, 2000.
30. Lenk P., Coult G., Damping of glass structures and components, Challenging Glass 2, Vol 2, 2010.
31. Carfagni M., Lenzi E., Pierini M., "The Loss Factor as a Measure of Mechanical Damping," Atti del 16th International Modal Analysis Conference, Santa Barbara, CA (USA), 2-5 febbraio 1998, Vol. 1, pp. 580-584